

**ADSORPTIVE REMOVAL OF INORGANIC POLLUTANTS FROM NUCLEAR POWER PLANT
WASTEWATER USING A MODIFIED ZEOLITE NANOCOMPOSITE**

A Major Qualifying Project Report

submitted to the Faculty

of the

WORCESTER POLYTECHNIC INSTITUTE

in partial fulfillment of the requirements for the

Degree of Bachelor of Science

By:

EDMUND CARL EDUAH

Date: March 7th, 2014

Approved by:

Professor Susan Zhou, Major Advisor

ACKNOWLEDGEMENT

I would like to first thank Worcester Polytechnic Institute and Shanghai Jiao Tong University for making this project and experience possible. I would also like to extend a special thank you to my advisors Professor Zhou and Professor Xu for their guidance and support and lastly to Timothy Wenzhong Zhang for assisting me throughout the experimental phase of the project.

ABSTRACT

This report focuses on the use of lab synthesized composite beads, made up of Xanthan Gum, Calcium Alginate and Na-A Zeolite, in adsorbing cobalt and nickel ions from nuclear power plant wastewater. The adsorption was investigated in a batch mode by changing relevant parameters including the adsorbent dosage, metal ions in solution, initial pH, temperature and salt concentration in the solution.

Optimal conditions for the adsorption process were found to be pH=5 and an adsorbent dosage of $\sim 2.0 \text{ g L}^{-1}$. The Pseudo-Second-order model best described the adsorption kinetics and the Langmuir isotherm model best fitted the adsorption process. Thermodynamically, the adsorption process was found to be spontaneous with a ΔG^0 of $-3237.45 \text{ KJ mol}^{-1}$ for cobalt and $-3494.93 \text{ KJ mol}^{-1}$ for nickel, and endothermic, with ΔH^0 being $5110.43 \text{ KJ mol}^{-1}$ for cobalt and $8251.67 \text{ KJ mol}^{-1}$ for nickel.

Finally, when tested in a synthesized solution of nuclear power plant wastewater, the XG-CA-Na-A composite beads showed encouraging results, removing 99.5% of the cobalt ions and 98.3% of the nickel ions in solution.

TABLE OF CONTENTS

ACKNOWLEDGEMENT	2
ABSTRACT	3
TABLE OF CONTENTS	4
LIST OF TABLES	6
LIST OF FIGURES	7
INTRODUCTION	8
BACKGROUND	9
INORGANIC POLLUTANTS OF INTEREST	9
CURRENT WASTEWATER TREATMENT METHODS FOR INORGANIC POLLUTANTS.....	10
<i>Chemical Precipitation</i>	10
<i>Membrane Filtration</i>	11
<i>Ultrafiltration (UF)</i>	11
<i>Reverse Osmosis</i>	12
<i>Nanofiltration</i>	12
<i>Electrodialysis (ED)</i>	13
<i>Adsorption</i>	14
<i>Choosing a Wastewater Treatment Method</i>	15
ADSORPTIVE REMOVAL OF WASTEWATER POLLUTANTS USING XG-CA-NA-A COMPOSITE BEADS	15
<i>Zeolites</i>	15
<i>Xanthan Gum and Calcium Alginate</i>	16
PURPOSE OF THIS PROJECT	17
OBJECTIVES.....	17
METHODOLOGY	18
MATERIALS AND INSTRUMENTS.....	18
METHOD.....	18
<i>Preparation of XG-CA-Na-A Beads</i>	18
<i>Batch Adsorption Procedure</i>	19
<i>Optimal conditions for the adsorption process</i>	19
<i>Kinetic Study</i>	20
<i>Isotherms and Thermodynamic Study</i>	21
<i>Study of Competing Effects</i>	23
RESULTS AND DISCUSSION	25
OPTIMAL ADSORPTION CONDITIONS.....	25
<i>Effect of XG-CA-Na-A composite beads dosage</i>	25
<i>Effect of pH</i>	26
ADSORPTION KINETICS	29
ISOTHERM AND THERMODYNAMIC STUDY.....	33
<i>Adsorption isotherms and temperature effects</i>	33
<i>Thermodynamics Studies</i>	35
COMPETING EFFECTS	37
<i>The effect of ionic Strength</i>	37
<i>Competition due to presence of both Nickel and Cobalt ions</i>	38
XG-CA-NA-A BEADS PERFORMANCE IN SYNTHESIZED NUCLEAR WASTEWATER.....	39
COMPARISONS BETWEEN XG-CA-NA-A BEADS AND OTHER PREVIOUSLY STUDIED ADSORBENTS.....	40

CONCLUSION	42
FUTURE PERSPECTIVES	42
REFERENCES	43
APPENDIX	46
APPENDIX A: PH OF PRECIPITATION FOR 15 MG L ⁻¹ COBALT AND NICKEL AQUEOUS SOLUTIONS.	46
<i>Cobalt solution</i>	46
<i>Nickel solution</i>	46

LIST OF TABLES

Table 1: Poisoning Effects and Groundwater QES for Co(II) and Ni(II) ions.....	10
Table 2: Composition of synthetic nuclear power plant wastewater.....	24
Table 3: Adsorption Capacity, Rate constant and regression values of the kinetic models	30
Table 4: Weber and Morris model constants for each adsorption step.....	31
Table 5: Adsorption isotherm constants and the regression values for the three experimented temperatures.....	35
Table 6: Thermodynamic constant values for the metal ions at all three temperatures studied.....	36
Table 7: The hydrated Ionic radii and Free energy of Hydration for the metal ions in solution.....	39
Table 8: Comparison between XG-CA-Na-A composite beads and other adsorbents in removing nickel ions from solution	40
Table 9: Comparison between XG-CA-Na-A composite beads and other adsorbents in removing cobalt ions from solution.....	41

LIST OF FIGURES

Figure 1: Chemical Precipitation Process Schematic.....	11
Figure 2: General Membrane Filtration Process Schematic	12
Figure 3: Electrodialysis Process Schematic	13
Figure 4: Adsorption Process Schematic	14
Figure 5A: Relationship between Adsorbent dosage and cobalt removed	25
Figure 5B: Relationship between adsorbent dosage and nickel removed	25
Figure 6A: Effect of pH on metal ion adsorption	26
Figure 6B: A comparison of the final system pH to the pH of precipitation of cobalt ions in solution	26
Figure 6C: A comparison of the final system pH to the pH of precipitation of nickel ions in solution	26
Figure 7A: Adsorption Kinetics for both metal ions	29
Figure 7B: Pseudo-first-order plots for both metal ions	29
Figure 7C: Pseudo-second-order plots for both metal ions	29
Figure 8A: Weber Morris Model plot for cobalt adsorption	31
Figure 8B: Weber Morris Model plot for nickel adsorption	31
Figure 9A: Cobalt Isotherm plots at 293K, 308K and 323K	33
Figure 9B: Nickel Isotherm plots at 293K, 308K and 323K	33
Figure 9C: Langmuir Isotherm Model plots for cobalt ion adsorption at 293K, 303K and 323K	33
Figure 9D: Langmuir Isotherm Model plots for nickel ion adsorption at 293K, 303K and 323K	33
Figure 9E: Freundlich Isotherm model plots for cobalt ion adsorption at 293K, 303K and 323K	34
Figure 9F: Freundlich Isotherm model plots for nickel ion adsorption at 293K, 303K and 323K	34
Figure 9G: Tempkin Isotherm model plots for cobalt ion adsorption at 293K, 303K and 323K	34
Figure 9H: Tempkin Isotherm model plots for nickel ion adsorption at 293K, 303K and 323K	34
Figure 10A: Plot of $\ln(C_s/C_e)$ vs. C_s for cobalt adsorption at the three test temperatures	36
Figure 10B: Plot of $\ln(C_s/C_e)$ vs. C_s for nickel adsorption at the three test temperatures	36
Figure 11A: Ionic Strength effect for cobalt adsorption	37
Figure 11B: Ionic Strength effect for nickel adsorption	37
Figure 12: A comparison between the amount of nickel ions and cobalt ions removed from solution when both ions are present in solution	38
Figure 13: Plot showing the percentage removal of all metal ions present in the synthetic nuclear power plant wastewater solution	39

INTRODUCTION

In industry today, there is a need for temperature control in various stages of the production process due to temperature requirements of different equipment that come together to make up the plant. In cases where temperature needs to be reduced, the most commonly used coolant is high purity water due to its affordability, high heat capacity and relative ease of disposal as compared to other fluids.

In nuclear power plants, electricity is generated from by steam turbines, nuclear fission, a process where atoms are split into smaller atoms with the release of large amounts of heat energy is used to create steam. During the nuclear fission process, many forms of radioactive materials are generated as a result of the splitting of the unstable atoms. These radioactive materials and hard metals seep into cooling water being used to keep the reactor within operation temperatures (*Nuclear Power Plant Radioactive Water Remediation*).

These hard metals and radioactive isotopes, in trace quantities will not be harmful to living organisms and are sometimes beneficial to the environment (*S. Rengaraj and Seung-Hyeon, 2002*). However, above permissible limits, these hard metals and radioactive materials can be extremely harmful to aquatic life and to other living organisms once ingested. (*Babel and Kurniawan, 2004*)

The dangers that these waste materials could cause to the environment have led to increased attention on finding efficient and economical methods for the removal of heavy metals and other radioactive materials from wastewater in the nuclear power industry.

Several methods exist for the removal of heavy metals from wastewater including chemical precipitation, membrane filtration, flotation, electrodialysis and adsorption.

This report focuses on the adsorption process, which has a competitive advantage to the other processes once a low cost sorbent is used. With that in mind, the project for which this report is based on investigates the use of a cheap, easily prepared nanocomposite beads created from a mixture of Zeolite A, Calcium Alginate and Xanthan Gum, as the adsorbent.

BACKGROUND

In nuclear power plant wastewater, there are trace quantities of several radioactive species. Most of these toxins present are heavy metals, with a few non-metallic species present as well. The background section introduces the inorganic pollutants of interest briefly, before delving into current wastewater treatment methods available. Once this has been completed, a more detailed depiction of the particular adsorption method of interest is given.

Inorganic Pollutants of interest

As suggested earlier, the major pollutant constituents of nuclear power plant wastewater are heavy metals. Heavy metals, defined loosely, are elements having atomic weights between 63.5 and 200.6, and a specific gravity greater than 5.0 (*Fu and Wang, 2011*). This definition covers a large range of elements however for the purposes of this project cobalt and nickel were given particular attention.

Cobalt is a hard ferromagnetic, silver-white, hard, lustrous, brittle element. It is needed in marine environment by nitrogen-fixing organisms like blue algae. In humans it is essential as it is part of vitamin B₁₂, which is essential to human health (Cobalt – Co, 2014). However in large quantities it can be detrimental to human health and aquatic life as shown in table 1.

Nickel, like cobalt, is a silvery white and hard element but differs from cobalt in that it is malleable and ductile. It is easily absorbed by organic matter, which explains why coal and oil contain considerable amounts. It appears in some beans as an essential enzyme and in tea as well (Nickel – Ni, 2014). However in large quantities it can be detrimental to human health as shown in table 1.

The ability of living organisms to absorb and accumulate these heavy metals makes it likely for these metals to exist beyond permitted concentrations in the living organism hence leading to various illnesses and disorders as shown in table 1.

Table 1: Poisoning Effects and Groundwater QES for Co(II) and Ni(II) ions

Heavy Metals	Effects of poisoning	Groundwater Enforcement (QES) (mg/L)	Quality Standards
Cobalt (Co ²⁺)	Heart, liver and thyroid Damage. May cause mutations.		0.04
Nickel (Ni ²⁺)	Dermatitis, nausea, chronic asthma, coughing, human carcinogen		0.10

(US EPA, 2013), (US DNR, 2012) and (S Rengaraj and Seung-Hyeon, 2002)

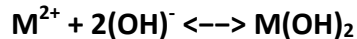
Due to the high solubility of heavy metals in aquatic environment they cannot be easily separated from wastewater and hence attention needs to be given to efficient separation methods.

Current Wastewater Treatment Methods for Inorganic Pollutants

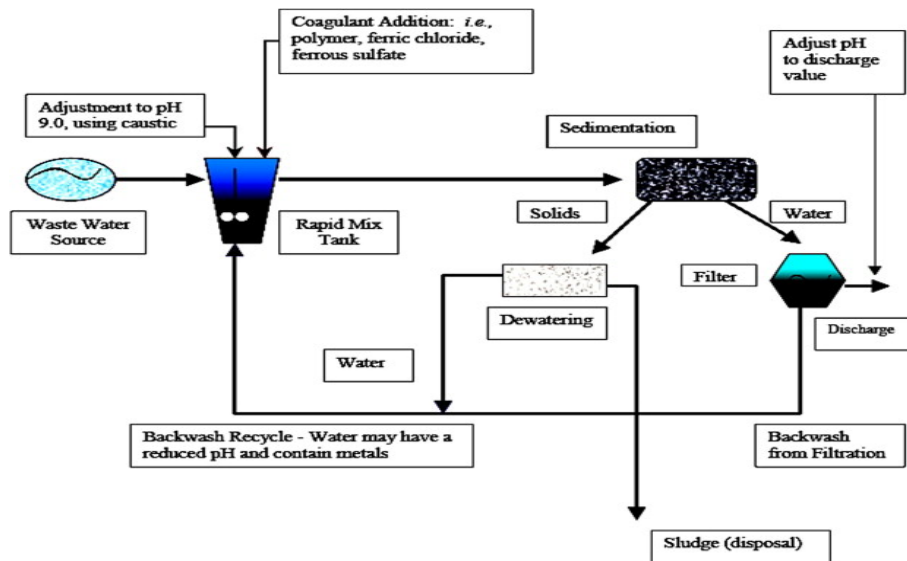
The danger posed by these toxins has led to considerable research into the separation of heavy metals and toxic non-metals from wastewater streams introduced below.

Chemical Precipitation

In this process a precipitant is used to remove dissolved metal ions in the wastewater stream by producing an insoluble metal hydroxide (*Barakat, 2011*).



The chemistry of this process suggests that one factor that will determine the cost of this process is the precipitant used. Lime and limestone are the most commonly used precipitants due to its availability and low cost (*Barakat, 2011*). The optimal pH for the process lies between 8-11.0 and the resulting metal hydroxides can be removed by flocculation or sedimentation (*Fu and Wang, 2011*). The high pH range along with the production of sludge, which has its own disposal problems, however presents some drawbacks to this treatment method (*Fu and Wang, 2011*).



(Wang et al, 2004)

Figure 1: Chemical Precipitation Process Schematic

Membrane Filtration

Membrane filtration is used to describe a group of treatment methods that make use of filtration methods. Depending on the size of the particle that needs to be retained, ultrafiltration, reverse osmosis, and micro or nano filtration can be employed for heavy metal removal from wastewater (Barakat, 2011).

Ultrafiltration (UF)

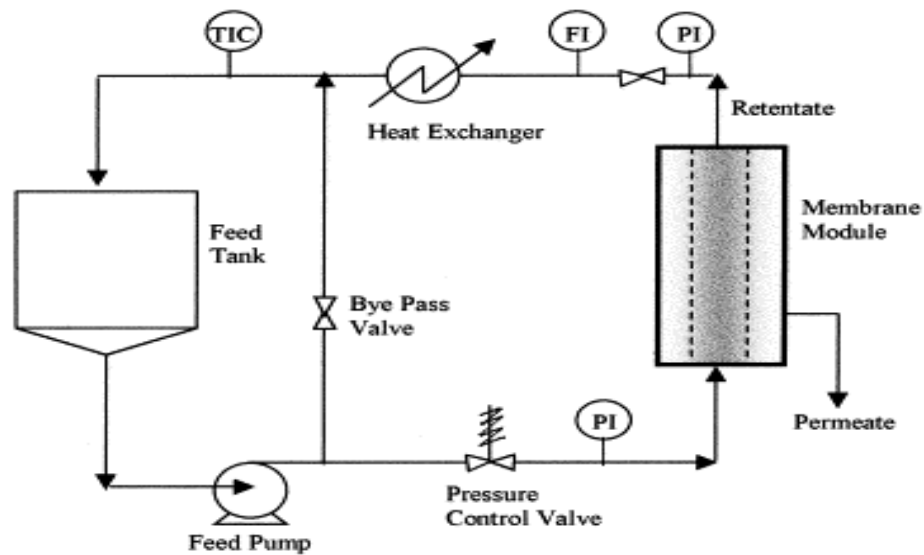
This is a low-pressure membrane process used to separate high molecular weight compounds from a liquid stream (Fu and Wang, 2011). The large pores used in this method results in ultrafiltration (UF) requiring fewer membrane elements and lower pressures however this also means that low molecular weight substances including heavy metals will pass through. Hence in order to increase the efficiency of the metal ion removal, the process is enhanced by the introduction of surfactants or water-soluble polymers, which form large metal-surfactant structures or macromolecular complexes respectively with the metallic ions. (Fu and Wang, 2011). These surfactants or polymers however add to the operating costs of the process. The membranes are also prone to fouling and radiation damage (Rahman et al, 2011).

Reverse Osmosis

In the reverse osmosis process, a semi-permeable membrane is used to allow fluid being treated through it while rejecting its contaminants with an efficiency of up to 99.5%. However its high power consumption due to pumping pressures and restoration of the membranes makes it a less favorable option (Fu and Wang, 2011).

Nanofiltration

Nanofiltration is the intermediate process between Ultrafiltration and Reverse Osmosis. It is a relatively easy to operate and reliable treatment method and has comparatively low energy consumption while maintaining high efficiency (Fu and Wang, 2011).



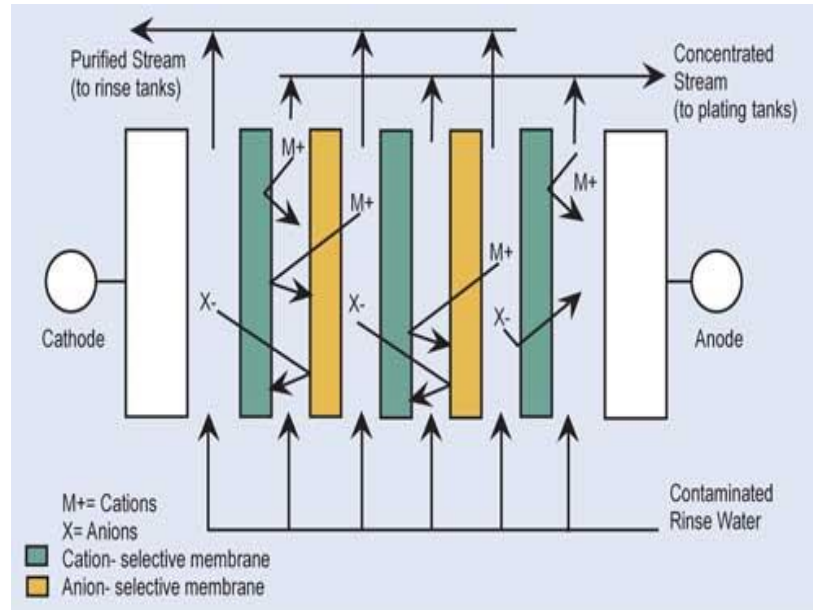
(Dhale and Mahajani, 2000)

Figure 2: General Membrane Filtration Process Schematic

Generally membrane filtration methods are highly efficient methods of removing heavy metal ions. However, as seen in the descriptions and schematic above, high costs, complexity and membrane fouling can make it an undesirable technique. Also low permeate flux makes the membrane filtration technique a slow treatment option on the industry level (Fu and Wang, 2011).

Electrodialysis (ED)

This process involves the separation of ions across charged membranes from one solution to another using an electric field as the driving force (*Fu and Wang, 2011*).



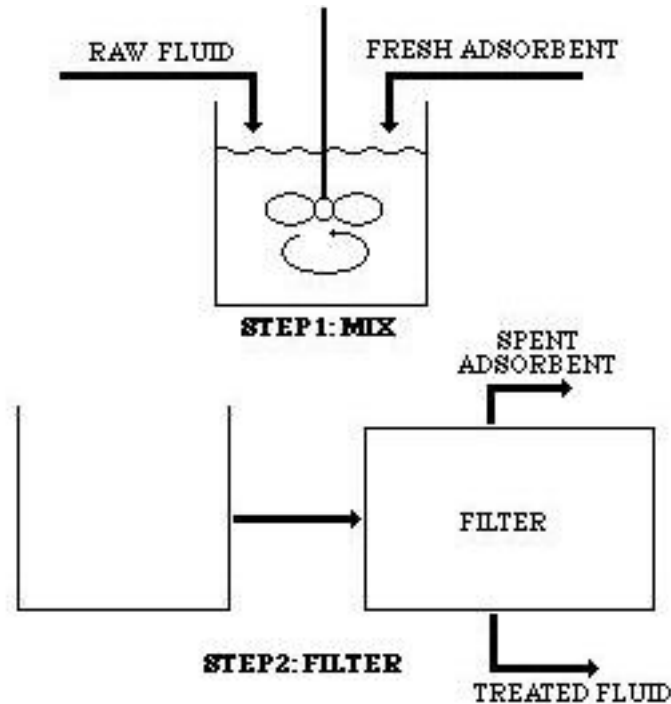
(Stephen R. Schulte, 2011)

Figure 3: Electrodialysis Process Schematic

In this treatment process, the contaminated wastewater is passed through cell compartments, which results in the anions migrating towards an anode and the cations migrating towards a cathode through anion exchange and cation exchange membranes. This movement results in the separation of the heavy metal ions from the wastewater stream as shown in figure 3.

Adsorption

Adsorption is a mass transfer process by which a substance is transferred from the liquid phase to the surface of a solid and becomes bound to the solid by physical and/or chemical interactions (Barakat, 2011). As the definition suggests, any solid that possesses the ability to attract the contaminants in the liquid phase onto its surface can be used as an adsorbent.



(Catalano et. al, 2005)

Figure 4: Adsorption Process Schematic

This makes the adsorption method a very flexible method as adsorbents can be chosen based on the contaminants present in the wastewater stream. Also the continued research into possibly cheaper adsorbents means that this method can become even more economically favorable than it is already.

Adsorption is also reversible, hence allowing adsorbents to be regenerated by suitable desorption processes and hence giving possibilities to reuse of adsorbents and reducing some of the costs associated with the treatment of wastewater by this method.

Other treatment methods such as photocatalysis exist but this method is for the treatment of organic waste in wastewater and hence does not apply to this project.

Choosing a Wastewater Treatment Method

As observed in the above background on the available wastewater treatment options, all options have their advantages and disadvantages. The most suitable procedure for any plant will therefore be dependent on the funds, needs and specifications of the particular plant that needs to treat its wastewater. Factors like initial metal concentration, wastewater components, operating costs, plant flexibility, reliability and environmental impact will need to be taken into consideration in making a decision on which treatment method to use (*Kurniawan et al., 2006*).

Adsorptive Removal of Wastewater Pollutants using XG-CA-Na-A composite Beads

As mentioned in the adsorption method description, any substance that possesses the ability to attract pollutants in the liquid phase onto its surface can be used as an adsorbent. In this project, the adsorbent that was studied was a lab-synthesized bead made out of a mixture of zeolite Na-A, Xanthan Gum (XG) and Calcium Alginate (CA).

Zeolites

Zeolites are crystalline materials made up of structures based on three-dimensional frameworks of alumina and silica tetrahedra. These typically anionic frameworks are populated by charge compensating cations to maintain neutrality. These compensating cations can participate in ion-exchange processes (*Price*). The polarity, shape and size selective properties of zeolites as a result of their tetrahedron framework and the ion-exchange ability of zeolites present attractive adsorbent possibilities for zeolites.

The loosely bound nature of extra-framework metal ions such as the Na ions means that they are often readily exchanged for other types of metal ions when in aqueous solution. In Zeolite Na-A, the zeolite used in this project, the charge compensating cation is Sodium and the zeolite has the molecular formula $\text{Na}_{12}((\text{AlO}_2)_{12}(\text{SiO}_2)_{12}) \cdot 27\text{H}_2\text{O}$. Hence in this project, it is expected that when present in aqueous solutions, the sodium ions will be exchanged out of the zeolite for hard metal ions such as Cobalt and Nickel present in the water.

Xanthan Gum and Calcium Alginate

Despite the attractive properties of zeolites for adsorption in wastewater treatment, their crystalline nature implies the need for a separation procedure after they have been introduced into the wastewater stream and this could possibly increase the operation costs of this method. This problem can however be solved, without affecting the ion exchange ability and the tetrahedron, by forming beads through the coating of the zeolites with natural polysaccharides (*Zhang et al, 2013*).

In this project, Xanthan gum, a common thickening agent, and Calcium Alginate, a water insoluble and gelatinous substance, are the polysaccharides used. Both polysaccharides are used in the food industry as emulsifiers and to increase viscosity. Most importantly, the water-insoluble nature property of Calcium Alginate makes it possible for the synthesized beads to be easily removed from the wastewater stream once the adsorption process is complete.

PURPOSE OF THIS PROJECT

Now that the wastewater treatment method of interest has been identified and described, the aim of this project will be to study the factors that affect the effectiveness of the adsorption process as well as the effectiveness of zeolites as adsorbents

Objectives

More specifically, the objectives of this project will be to:

1. Find the optimal conditions for the adsorption process.
 - A. Effect of adsorbent dosage on the adsorption process.
 - B. Effect of pH on adsorption process.

2. Investigate the adsorption capacity of the zeolites for different kinds of heavy metal ions using flame atomic adsorption spectrometry and inductive coupled plasma optical emission spectrometry.
 - A. Find the kinetics of the adsorption process
 - B. Perform a thermodynamic study of the adsorption process
 - i. Find the effect of temperature on the adsorption process.
 - ii. Analyze adsorption isotherms.

3. Find the effect of competing adsorbates in the wastewater on the adsorption process.
 - A. Competition due to presence of background electrolytes.
 - B. Competition due to multiple metal ion presence.
 - C. Find the behavior of adsorbent in synthesized nuclear power plant wastewater.

METHODOLOGY

Materials and Instruments

The XG-CA-Na-A beads, synthesized in the lab, were used as the adsorbent for all of the batch adsorption experiments carried out in this project. In all of the tests, the performance of the beads in adsorbing Ni^{2+} and Cu^{2+} ions, the adsorbates, was studied by the use of Flame Atomic Adsorption Spectroscopy or, in the case of latter experiments, Induced Coupled Plasma Optical Emission Spectroscopy. The pH of all solutions was controlled using diluted Nitric Acid (HNO_3) or Sodium hydroxide (NaOH).

Method

Preparation of XG-CA-Na-A Beads

First, a desired amount of dried zeolite Na-A (meshed through 50-screen sieve) was re-suspended in water under stir and ultrasonication to create a 33% weight percent zeolite solution. Then, 1 % (w/w) sodium alginate (SA) (190 cps viscosity) was prepared by mixing the SA with water under ultrasonication. 0.5% (w/w) Xanthan gum (XG) was also prepared by mixing XG powder with water under stir and ultrasonication. Lastly, a 0.2 mol L^{-1} solution of Calcium Chloride was prepared.

The solution that makes up the Zeolite beads is then prepared in a gram ratio of 1g of zeolite solution to 6g of 1% sodium alginate solution to 10g of 0.5% Xanthan gum solution. It is important to note that the solution must be created in the given order, the sodium alginate is added to the zeolite A solution before the xantum gum solution is added to the previous mixture. It is also important to know that at each point of solution preparation and mixing, thorough mixing must be achieved by use of a stirrer and all air bubbles must be removed by using an ultrasound shaker.

Using an injector, the Zeolite A-sodium Alginate-Xantum gum mixture is then added drop wise to the calcium chloride solution to obtain the desired beads. The beads are kept overnight in the calcium chloride solution and the filtered and thoroughly washed with D.I water. Once that is done, they are placed on a plate in one layer and placed in an oven at 60°C overnight.

Batch Adsorption Procedure

During the batch adsorption process, 25 ml of metal solution at initial concentration 15 mg L⁻¹ was placed in a sample flask and the pH was adjusted to a desired pH by using dilute and little amounts of HNO₃ or NaOH. A specific dosage of the composite beads was then added into the flask and left on an orbital shaker at 120 rpm for a specific period of time. Finally, the sample solutions are decanted out and if necessary diluted before the FAAS or ICPOES was used to determine the metal concentration in the supernatant.

The concentration values are then used to calculate the adsorption capacity (q_e) and/or distribution coefficient (K_d) from the equations below:

$$q_e = \frac{C_o - C_e}{m} \times V \quad (1)$$

Adsorption capacity equation

$$K_d = \frac{(C_o - C_e)}{C_e} \times \frac{V}{m} \quad (2)$$

Distribution coefficient equation

Distribution coefficient data implicitly indicate the selectivity, capacity, and affinity of an ion for ion exchange. Based on the results obtained, conclusions were drawn on the capabilities of the beads or the effect of certain condition changes on the performance of the beads.

The batch adsorption procedure was used in all the studies carried out on the performance of the XG-CA-Na-A beads.

Optimal conditions for the adsorption process

Optimal Dosage

In order to find the optimal conditions for the adsorption process, experiments were carried out to find the optimal dosage and pH for the adsorption process. First the batch adsorption procedure was carried out under a pH of 5 but with different adsorbent amounts for each run. The adsorbent amounts used were 0.025g, 0.05g, 0.075g and 0.1g. Each experiment was triplicated to validate results. The q_e and K_d values obtained

from the above experiments were used to determine the optimal dosage for the adsorption process.

Optimal pH and pH effect

Once this had been achieved, another set of batch adsorption experiments were carried out, this time using the optimal adsorbent amounts determined in the first set of experiments and varying the pH for each run. A pH range of 3-9 was tested and the resulting q_e and K_d values were used to determine the optimal pH and the effect of pH on the adsorption process.

Once the optimal pH and dosage were obtained, they were used as the pH and dosage in all of the other studies carried out during the project.

Kinetic Study

The kinetic study was performed using 25 ml of solution with an initial metal concentration of 15 ppm and ~0.05g of adsorbent. The bottles were agitated at 120 rpm at ~23°C. Samples were withdrawn for analysis by the FAAS at periods of 5, 10, 15, 20, 30, 40, 50, 60, 90, 120, 180, 240, 300, 360, 420, 480 minutes and one sample was withdrawn after being left overnight.

To determine which kinetic model best described the adsorption process, the results obtained were used to generate plots for the Pseudo-first-order kinetics model proposed by Lagergen (*Hui et al, 2005*), which has a general equation:

$$\log(q_e - q_t) = \log(q_e) - \frac{k_1}{2.303} t \quad (3)$$

Pseudo-first-order kinetics model equation

and the Pseudo-second-order kinetic model developed by Ho and McKay (*Hui et al, 2005*), which has the equation:

$$\frac{t}{q_t} = \frac{1}{k_2 q_e^2} + \frac{1}{q_e} t \quad (4)$$

Pseudo-second-order kinetic model equation

Hence by plotting graphs of $\log(q_e - q_t)$ vs. t and t/q_t vs. t , the model which best described the particular adsorption process in the project was identified and the appropriate rate constants were determined.

After the more suitable kinetic model was determined, the Weber and Morris model was used to describe the intra-particle diffusion that occurs in the adsorption process. The equation needed in order to do this is:

$$Q_t = K_i t^{0.5} + I \quad (5)$$

Weber and Morris Model equation

(S. Zhang et al, 2013)

If the Q_t against $t^{0.5}$ plot exhibits a straight line and passes through the origin, the adsorption process is controlled by intra-particle diffusion only. However, if the plot divides into three distinct segments, then two or more steps influence the adsorption process (Srivastava et al, 2006).

Isotherms and Thermodynamic Study

Isotherm Study

The isotherm and thermodynamic study were performed using 25 ml solutions of different initial metal concentrations ranging from 10 - 400 ppm with ~0.05g of adsorbent placed in the solutions. The bottles were agitated at 120 rpm and the experiments were repeated at three different temperatures (20, 35 and 50 °C).

Comparison with Langmuir, Freundlich and Tempkin Isotherm models was made using the following equations obtained from available literature (Foo and Hameed, 2010):

$$\frac{C_e}{q_e} = \frac{1}{bQ_0} + \frac{C_e}{Q_0} \quad (6)$$

Langmuir Isotherm Model linear equation

$$\log(q_e) = \log(K_F) + \frac{1}{n} \log(C_e) \quad (7)$$

Freundlich Isotherm Model linear equation

$$q_e = \left(\frac{RT}{b_T}\right) \ln(A_T) + \left(\frac{RT}{b_T}\right) \ln(C_e) \quad (8)$$

Tempkin Isotherm Model Linear equation

By comparing the experimental results to the above equations, the most accurate model that described the adsorption process was identified and the maximum adsorption capacity of the XG-CA-Na-A beads was found.

Thermodynamic study and Temperature effects

The results obtained were also used to generate a q_e vs. C_e plot for each of the temperatures studied in order to adequately investigate the effect of temperature on the adsorption process.

In addition to this, the adsorption thermodynamics was studied from the results obtained from this set of experiments. The thermodynamic equilibrium constant is defined as:

$$K_0 = \frac{v_s \cdot C_s}{v_e \cdot C_e} \quad (9)$$

Thermodynamic equilibrium constant equation

where v_s and v_e are the corresponding activity coefficients, C_s is the amount of metal ion absorbed per unit mass of the composite and C_e is the concentration of metal ion in the liquid phase at equilibrium. K_0 was obtained from extrapolating C_s to zero in the plot of $\ln(C_s/C_e)$ vs. C_s (S Zhang et al, 2013). This K_0 value was then used to calculate the change in standard Gibbs free energy (ΔG^0 , KJmol^{-1}) using the equation:

$$\Delta G^0 = -RT \ln(K_0) \quad (10)$$

Standard State Gibbs Free energy of reaction at Equilibrium equation

(C. Luo et al, 2013)

The change in enthalpy and entropy were also calculated using the following equations:

$$\ln K_{0(T2)} - \ln K_{0(T1)} = -\frac{\Delta H^0}{R} \left(\frac{1}{T_2} - \frac{1}{T_1} \right) \quad (11)$$

Van't Hoff Equation

(D. Mohan and K.P. Singh, 2002)

$$\Delta S^0 = -\frac{(\Delta G^0 - \Delta H^0)}{T} \quad (12)$$

Entropy equation derived from Gibbs free energy of reaction equation

(D. Mohan and K.P. Singh, 2002)

The results from these equations were then used to draw conclusions on the spontaneity of the adsorption process as well as whether the process is endothermic or exothermic.

Study of Competing Effects

Competition due to presence of background electrolytes

The presence of background electrolytes may affect the adsorption of the Co^{2+} and Ni^{2+} ions by the XG-CA-Na-A composites in aquatic media. In order to test this effect batch adsorption experiments were run with $\sim 0.05\text{g}$ of adsorbent added to 25 ml solutions containing ~ 15 ppm of metal ion and varied concentrations of NaCl, KCl, MgCl_2 and CaCl_2 (0.0025-0.1000M). The resulting concentrations were obtained using the FAAS and conclusions drawn based on these results.

Competition due to presence of both Nickel and Cobalt ions

The adsorption of the metal ions by the XG-CA-Na-A composite beads was also studied in the scenario where both metal ions are present in the aqueous solution. This presence of both metal ions may affect the adsorption capacity due to competition for adsorption space. In order to test this effect, batch adsorption experiments were run with $\sim 0.05\text{g}$ of adsorbent added to 25 ml solutions containing varied concentrations of both metal ions (10 ppm – 50 ppm). Batch adsorption experiments were also run with $\sim 0.05\text{g}$ of adsorbent added to 25 ml solutions containing only one of the two metal ions being studied at the same range of concentrations (10 ppm – 50 ppm). The resulting concentrations obtained from FAAS were used to draw conclusion on the competing effects of the coexisting metal ions in the aqueous media.

Simulated nuclear power plant waste water

To investigate how the XG-CA-Na-A composite beads will fair in real life situation, batch adsorption experiments were run with about $\sim 2.0\text{g}$ of adsorbent with a litre of metal ion solution containing various heavy metals at various concentrations obtained from literature (*Rengaraj and Seung-Hyeon, 2002*). The concentration and metal ion present in the solution are presented in table 2 below.

Table 2: Composition of synthetic nuclear power plant wastewater

Compound	Concentration (mg L ⁻¹)
Co(NO ₃) ₂ · 6H ₂ O	1
Ni(NO ₃) ₂ · 6H ₂ O	15
Fe(NO ₃) ₃ · 9H ₂ O	30
Sb ₂ O ₅	5
AgNO ₃	5
H ₃ BO ₃	20
Cr(NO ₃) ₃ · 9H ₂ O	4
LiOH · H ₂ O	0.5
CsNO ₃	0.5

(Rengaraj and Seung-Hyeon, 2002)

RESULTS and DISCUSSION

Optimal Adsorption Conditions

Effect of XG-CA-Na-A composite beads dosage

As shown in figures 5A and B, the adsorption efficiency increases as the adsorbate dosage increases. The graphs suggest that the removal efficiency increased to about 99% for both metal ion solutions when the adsorbate dosage was at ~ 2.0 g/L.

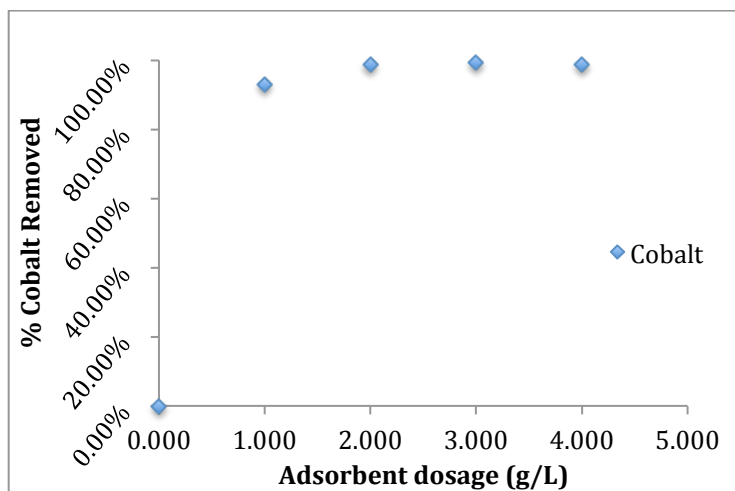


Figure 5A: Relationship between XG-CA-Na-A composite beads and amount of cobalt removed from the system.

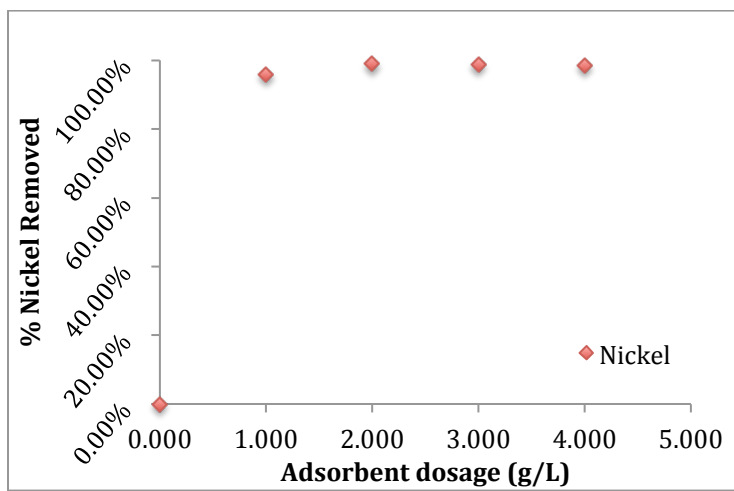


Figure 5B: Relationship between XG-CA-Na-A composite beads and amount of nickel removed from the system.

It was also observed that as the adsorbent dosage exceeded ~ 2.0 g/L, the adsorption efficiency reached a saturation point. The initial increase in the adsorption efficiency can be attributed to the increase in the surface area of the adsorbent and the availability of adsorption sites as the adsorbent dose increases. However, after a while, this increasing effect is cancelled as due to overlapping or aggregation of adsorption sites, which results in a decrease or no effective increase in the total adsorbent surface area (Kilic et al, 2013).

Effect of pH

According to the results in figure 6A, as the initial pH of the system increases within the acidic region, the metal ion removal efficiency increases. Once the pH of the system moves into basic region the increasing pH effect decreases and eventually the adsorption efficiency begins to decrease.

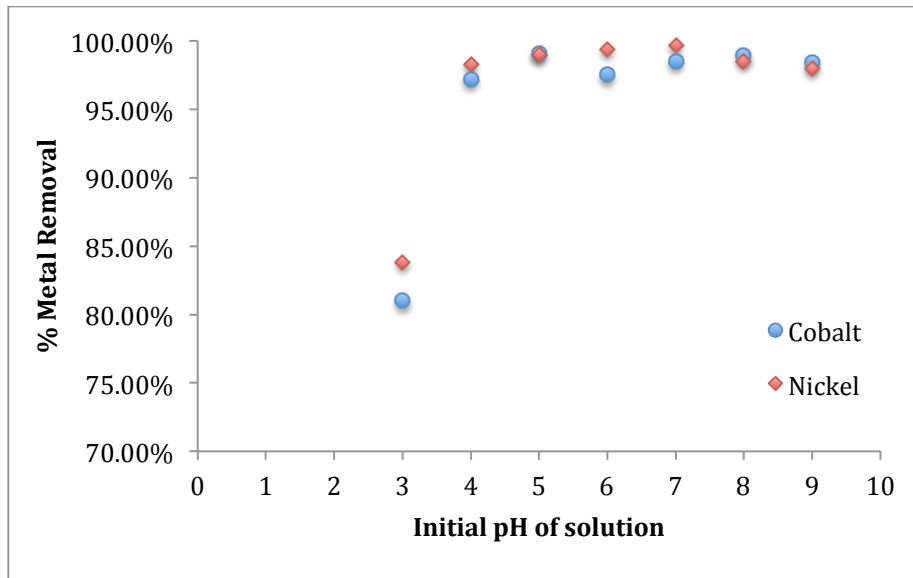


Figure 6A: Effect of pH on metal ion adsorption.

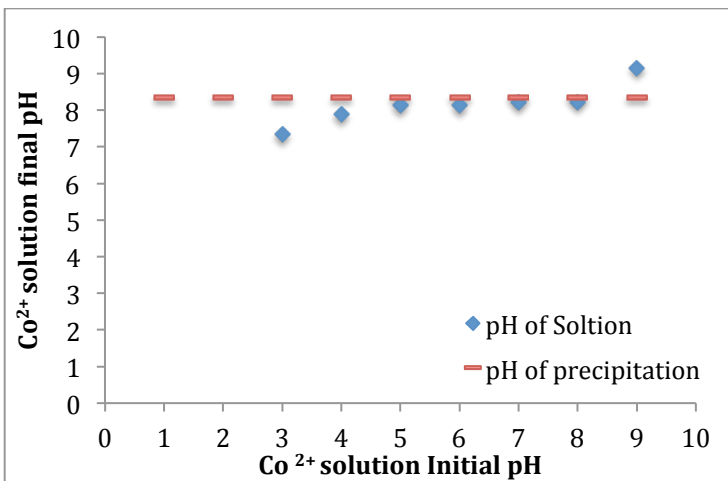


Figure 6B: A comparison of the final system pH to the pH of precipitation of cobalt ions in solution.

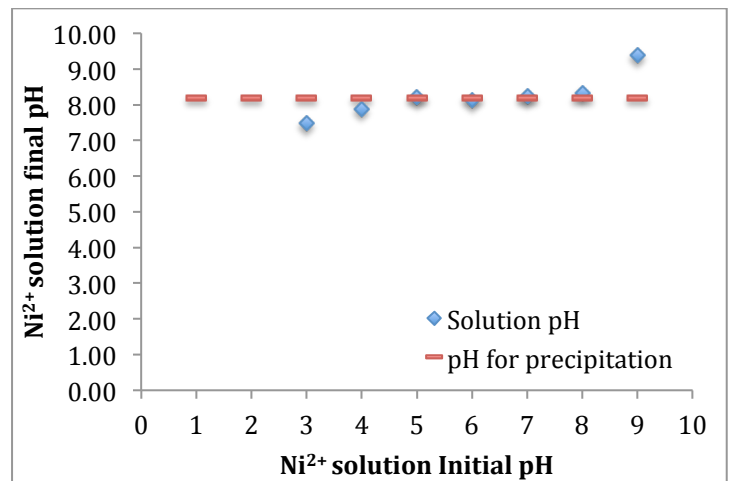


Figure 6C: A comparison of the final system pH to the pH of precipitation of nickel ions in solution.

In terms of optimal pH, as represented in figure 6A, the maximum uptake of Ni²⁺ ions occurred at a pH of 7, although the difference between adsorption efficiencies at pH of 5,6, and 7 is almost insignificant. For Co²⁺, the maximum adsorption efficiency was obtained at a pH of 5.

In an attempt to explain the effect of the initial pH of the system on the adsorption process, the results obtained at initial pH of 9 were not taken into consideration, as they do not reflect the adsorption efficiency accurately. Based on the K_{sp} values of Ni²⁺ and Co²⁺ (*Solubility Product Constants*), it is expected that some precipitation will begin to occur after pH values of 8.19 for the Ni²⁺ solution and 8.35 for the Co²⁺ solution (Refer to appendix A for calculation). As shown in figure 6B and 6C, the final pH of the systems when the initial pH is 9 is significantly above the precipitation pH. Hence, results obtained for the effect of pH at a pH of 9 were not taken into account because at this operating pH significant precipitation occurs affecting the adsorption efficiency value reported.

That being said, the effect that the initial pH has on the adsorption process can be explained by ion competition in the acidic phase and by the formation of hydroxyl complexes in the basic region. The presence of H⁺ (or H₃O⁺) at pH values below 7 means that there is competition for adsorption spaces between the metal ions and the H⁺ ions. (Hui et al, 2005) This competition is greater with lower pH values and the presence of more H⁺ ions. Hence, as the pH value increases from 3 – 7, the amount of H⁺ ions present decreases which results in less competition for available adsorption spaces and hence leads to an increase in efficiency of the adsorption process.

Also, as the pH value increases from 7 – 9, the presence of inorganic ligands like OH⁻ increases and therefore may result in the formation of hydroxyl complexes, which will in turn affect the amount of metal ions available for adsorption. (*S. Rengaraj and Seung-Hyeon, 2002*) As a result, more metal ions remain in solution after the adsorption process, hence explaining the downward trend noticed from pH 7-9.

Finally, it was observed that the pH of the solution before and after the addition of the adsorbate varied when the initial pH of the system was below pH values of 8 as

shown in figure 6B and 6C. This difference can be attributed to the alginate adsorbent forming a weak base that neutralizes the acidic solution (*Ruiz et Al, 2013*). This also explains why the effect was not observed when the initial pH of the system was 8 or 9.

As a result an adsorbate dosage of ~ 2.0 g/L and a system pH of 5 was used for the rest of the experiment as these conditions are expected to yield maximum or close to maximum adsorption efficiencies.

Adsorption Kinetics

The kinetic study of the adsorption process in the case of both metal ions is important because it helps in explaining the interactions between the targeted metal ions and the XG-CQ-Na-A composite beads. The influence of contact time on the metal ion adsorption as well as the linear plots of the pseudo-first- and pseudo-second-order kinetics are shown in figures 7A to C.

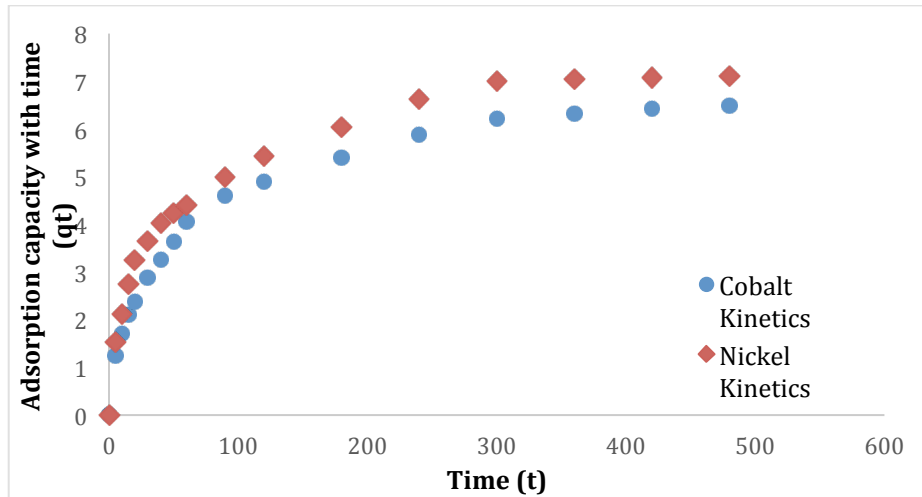


Figure 7A: Adsorption Kinetics for both metal ions

Based on figure 7A, the equilibrium time of Co^{2+} adsorbed on the XG-CA-Na-A composites was ~ 480 minutes while for Ni^{2+} , the equilibrium time was ~ 420 minutes.

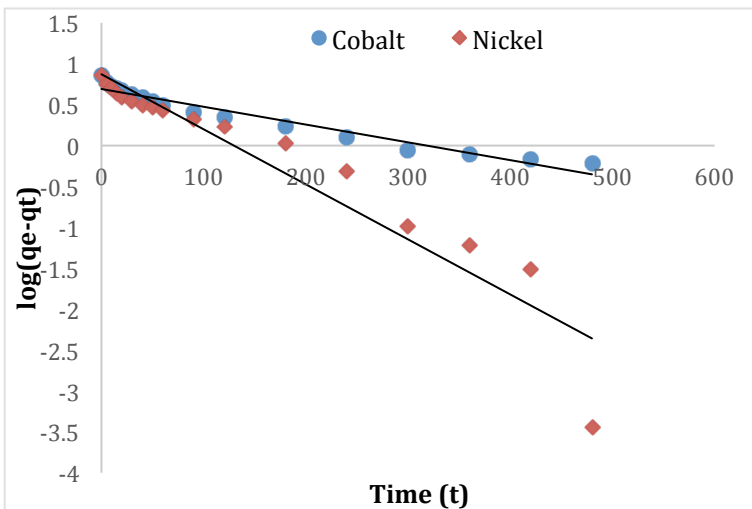


Figure 7B: Pseudo-first-order plots for both metal ions.

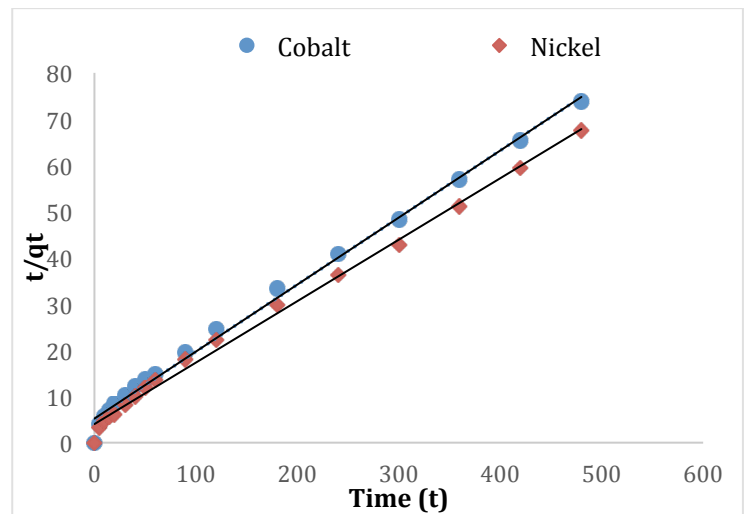


Figure 7C: Pseudo-second-order plots for both metal ions.

Also, the pseudo-second-order plots show considerably good linearity with R^2 values above 0.99 for both Nickel and Cobalt plots as compared to the R^2 values for the pseudo-first-order plots, which were 0.90 and 0.95 for Nickel and Cobalt respectively. This implied that the adsorption kinetics of the XG-CA-Na-A composites followed the pseudo-second-order model. The Rate constants are shown in table 3 below.

Table 3: Adsorption Capacity, Rate constant and regression values of the kinetic models

Species	q_e (exp) (mg g ⁻¹)	Pseudo-first-order model			Pseudo-second-order model		
		q_e (mg g ⁻¹)	K1 (min ⁻¹)	R2	q_e (mg g ⁻¹)	K2 (g mg ⁻¹ min ⁻¹)	R2
Nickel	7.11	7.4456	0.0154	0.903	7.4405	0.0042	0.991
Cobalt	6.51	4.9170	0.0051	0.948	6.7659	0.0040	0.994

During the adsorption process, three consecutive steps may take place (S. Zhang et al, 2013):

- Transport of adsorbate ions to the external surface of adsorbent (Film Diffusion)
- Transport of adsorbate ions within the pores of adsorbent (Particle Diffusion)
- Adsorption of the adsorbate ions on the interior surface of the adsorbent.

The third step is a non-limiting step. However, during the adsorption process, the film diffusion and the particle diffusion or only one of these steps limits the adsorption rate and the Weber and Morris model is used to determine this (S. Zhang et al, 2013).

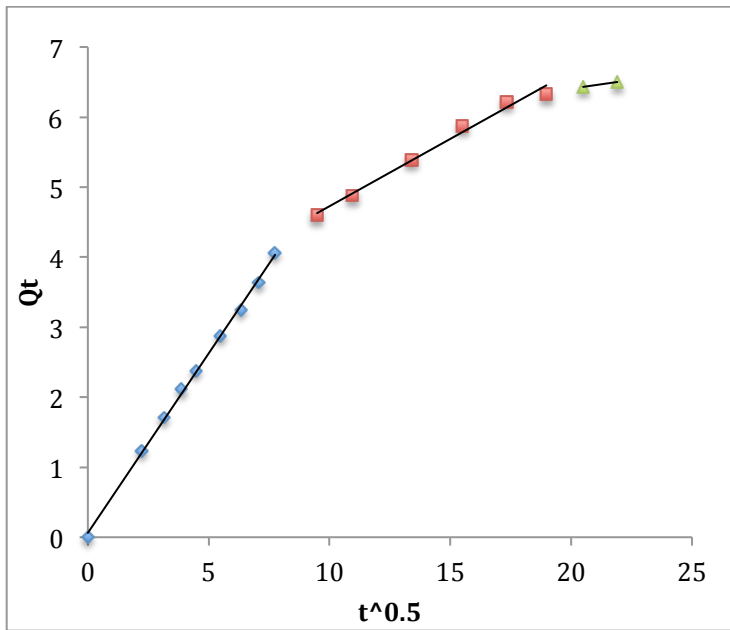


Figure 8A: Weber and Morris model plot for cobalt adsorption.

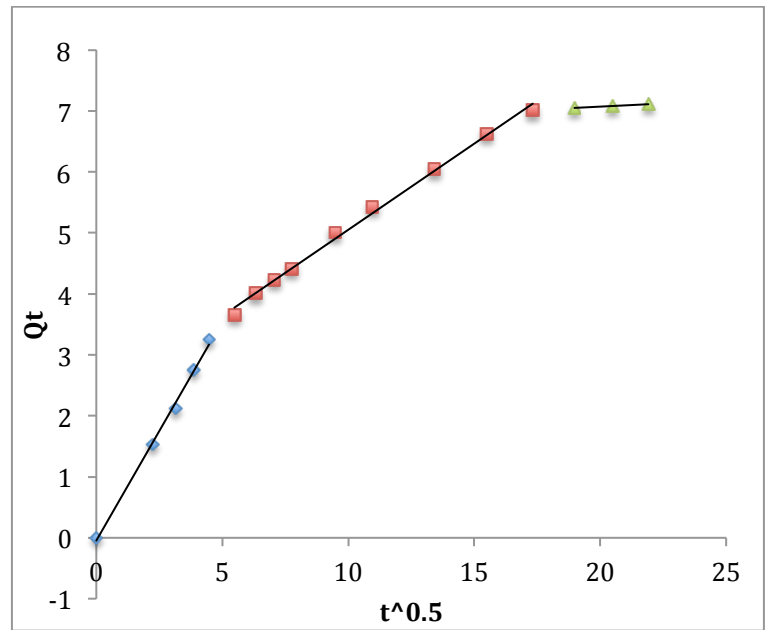


Figure 8B: Weber and Morris model plot for nickel adsorption.

The Q_t against $t^{0.5}$ plots shown in figures 8A and 8B show three distinct linear segments, which therefore suggests that both the film diffusion and particle diffusion steps limit the adsorption rate of the adsorption process. The rate constants for each of the three steps are shown in table 4 below.

Table 4: Weber and Morris model constants for each adsorption step.

Step	Constants	Species	
		Co ²⁺	Ni ²⁺
Film Diffusion	K_1 (mg g ⁻¹ min ⁻¹)	0.5127	0.7188
	I	0.0617	0.0455
	R^2	0.9988	0.9964
Particle Diffusion	K_1 (mg g ⁻¹ min ⁻¹)	0.1924	0.2825
	I	2.8042	2.2265
	R^2	0.9872	0.9959
Equilibrium	K_1 (mg g ⁻¹ min ⁻¹)	0.0495	0.0206
	I	5.4183	6.6579
	R^2	1	0.9998

Based on table 4, it was observed that the Nickel adsorption process had faster rate constants than the Cobalt adsorption process until adsorption is reached. This faster

rate compliments results shown in table 3, which suggest that the adsorption capacity of nickel is greater than that of cobalt.

Also, the K_1 values in the equilibrium step were expected to be zero. However, the results suggest that the adsorption process was not necessarily at equilibrium yet. This could be a possible explanation for the disparity between the experimental adsorption capacities and the expected adsorption capacities under the pseudo-second-order model as shown in Table 3.

Isotherm and Thermodynamic study

Adsorption isotherms and temperature effects

The adsorption isotherms for Co^{2+} and Ni^{2+} were studied at 20, 35, 50 °C as shown in figures 9a-h. As table 5 clearly shows, the adsorption isotherms for both metal ions were best described by the Langmuir isotherm model.

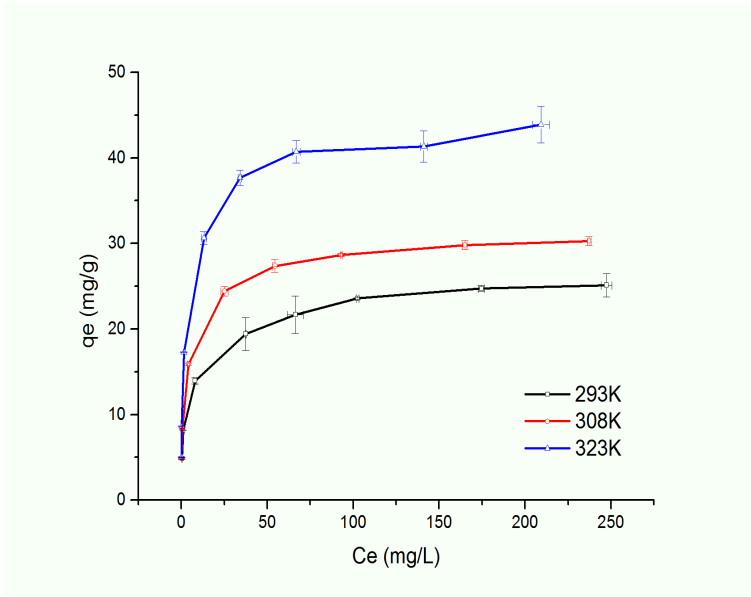


Figure 9A: Cobalt Isotherm plots at 293K, 308K and 323K.

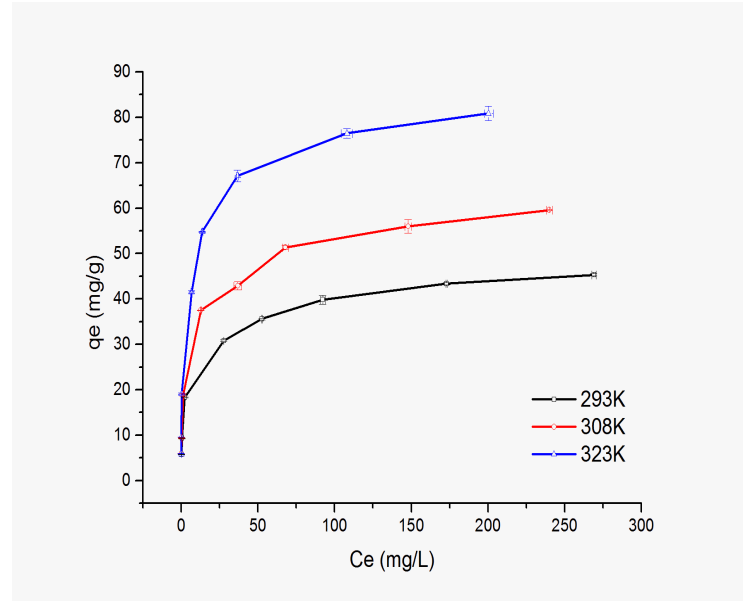


Figure 9B: Nickel Isotherm plots at 293K, 308K and 323K.

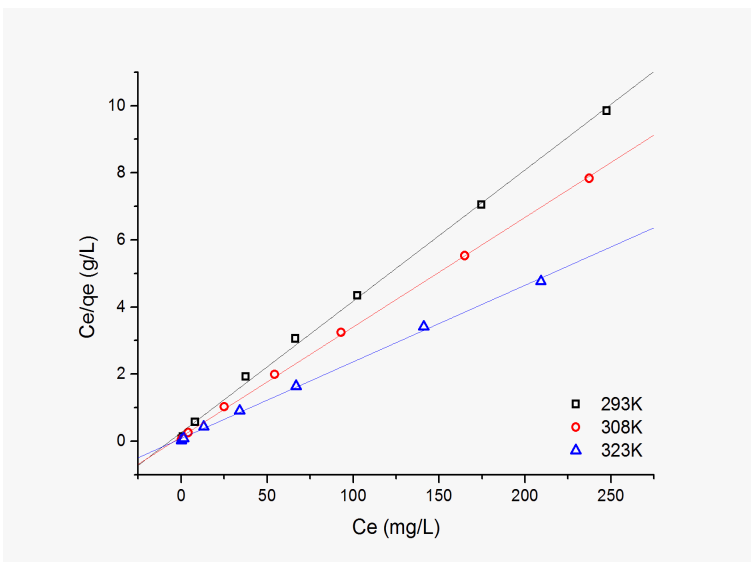


Figure 9C: Langmuir isotherm model plots for cobalt ion adsorption at 293K, 308K and 323K.

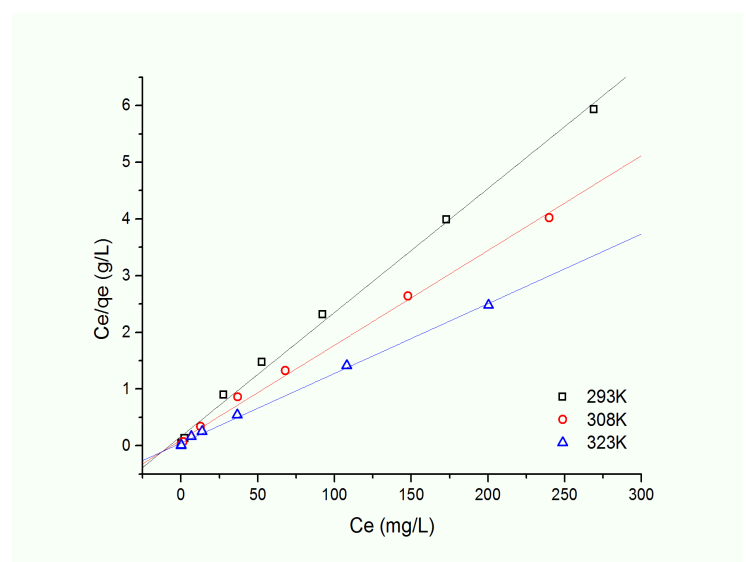


Figure 9D: Langmuir isotherm model plots for nickel ion adsorption at 293K, 308K and 323K.

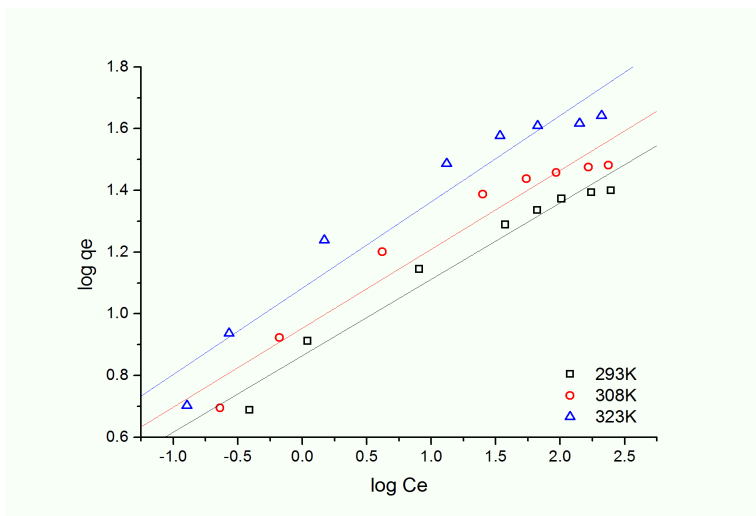


Figure 9E: Freundlich Isotherm model plots for cobalt ion adsorption at 293K, 303K and 323K

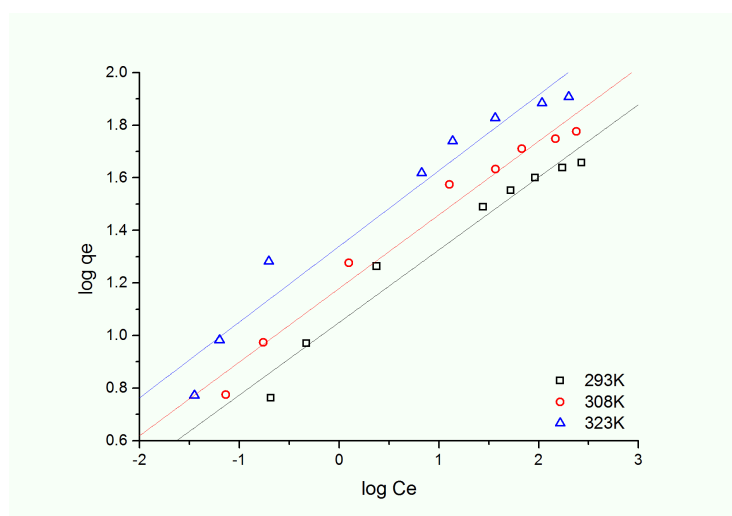


Figure 9F: Freundlich Isotherm model plots for nickel ion adsorption at 293K, 303K and 323K

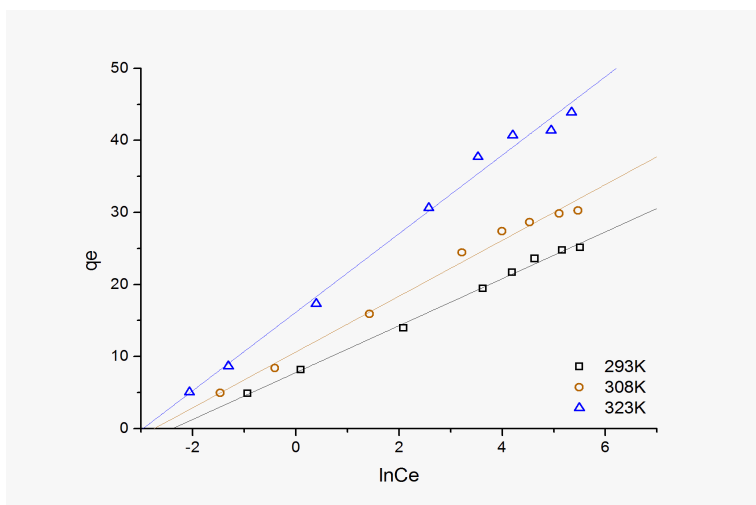


Figure 9G: Tempkin Isotherm model plots for cobalt ion adsorption at 293K, 303K and 323K.

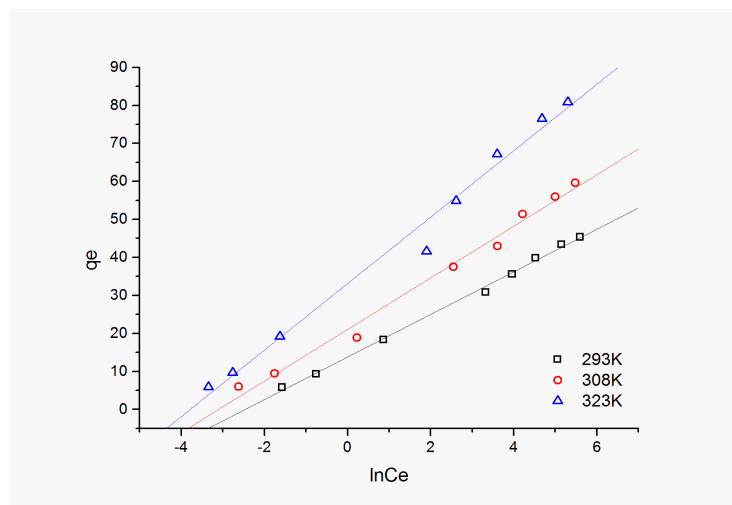


Figure 9H: Tempkin Isotherm model plots for nickel ion adsorption at 293K, 303K and 323K.

The Langmuir isotherm model is based on the assumption that the adsorption process is a monolayer process (*Foo and Hameed, 2010*). Therefore our results verify that the adsorption of the Ni^{2+} and Co^{2+} ions by the XG-CA-Na-A composites was a monolayer adsorption process.

Table 5: Adsorption isotherm constants and the regression values for the three experimented temperatures

				Species			
Co ²⁺				Ni ²⁺			
Temperature (K)	Isotherm Model			Temperature (K)	Isotherm Model		
				LANGMUIR ISOTHERM MODEL			
				Constants			
	q_m	b	R^2		q_m	b	R^2
293	25.5754476	0.151081917	0.99813	293	45.6621005	0.13240629	0.99637
308	30.5810398	0.249427918	0.99941	308	59.8802395	0.16534653	0.99609
323	43.8596491	0.283935243	0.9985	323	81.300813	0.2639485	0.99785
				FREUNDLICH ISOTHERM MODEL			
				Constants			
	K_F	n	R^2		K_F	n	R^2
293	7.31475863	4.037141704	0.96712	293	11.2227684	3.62187613	0.96323
308	8.83222248	3.909304144	0.94607	308	15.1147163	3.57270454	0.97391
323	12.1143467	3.573981415	0.9399	323	21.8574755	3.47342827	0.95322
				TEMPKIN ISOTHERM MODEL			
				Constants			
	RT/b_T	A_T	R^2		RT/b_T	A_T	R^2
293	3.2548	10.90954734	0.9967	293	5.6061	11.6714215	0.99725
308	3.8724	15.5897748	0.99048	308	6.7899	22.1499316	0.98915
323	5.4488	19.39932086	0.99154	323	8.7481	43.9924984	0.98626

According to the Langmuir isotherm model. The maximum adsorption capacity of the XG-CA-Na-A composites for Co²⁺ was 25.58, 30.58 and 43.86 mg g⁻¹ at 20,35 and 50 °C respectively. For Ni²⁺, the maximum adsorption capacity for the XG-CA-Na-A composites was 45.66,59.88 and 81.30 mg g⁻¹ at 20,35 and 50°C respectively. Hence the Langmuir isotherm model suggests that composite is more selective to Nickel than it is to Cobalt. The increase in adsorption capacity also suggests that as the temperature increases the adsorption capacity also increases.

Thermodynamics Studies

The increase in adsorption capacity as the temperature increases indicates that the adsorption process is an endothermic reaction. The equilibrium constant (K_o) values provided in table 6 were derived from extrapolating the $\ln(C_s/C_e)$ vs. C_s plot, shown

in figure 10a and b, to the y-axis. Clearly, as the temperature increases, the K_0 value increases signifying that the amount of metal ion adsorbed per unit mass of adsorbent increases.

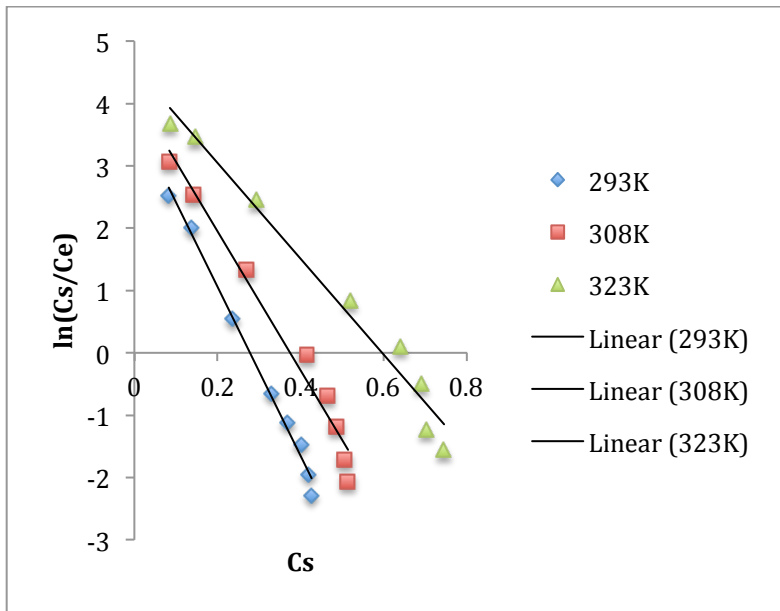


Figure 10A: Plot of $\ln(C_s/C_e)$ vs. C_s for cobalt adsorption at the three test temperatures.

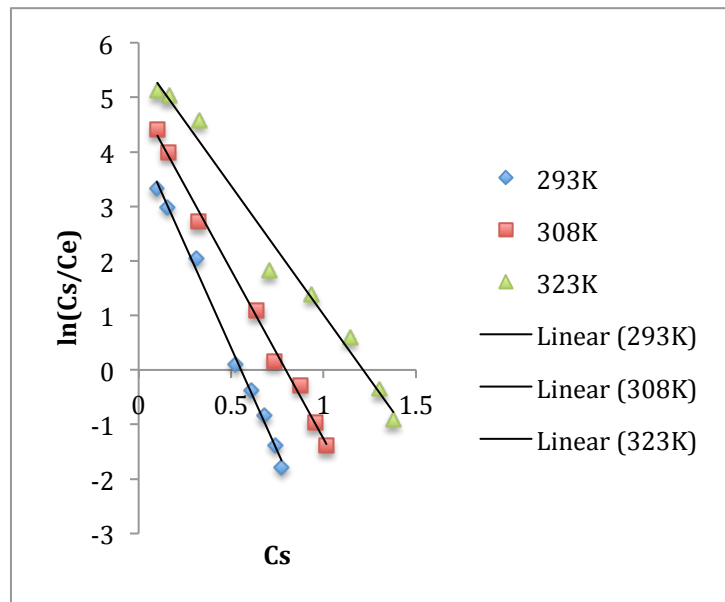


Figure 10B: Plot of $\ln(C_s/C_e)$ vs. C_s for nickel adsorption at the three test temperatures.

Using the K_0 values obtained, the ΔG^0 , ΔH^0 , and ΔS^0 of the adsorption process at the various temperatures was found as shown in table 6.

Table 6: Thermodynamic constant values for the metal ions at all three temperatures studied.

Thermodynamic Constant	Temperature (K)					
	Ni ²⁺			Co ²⁺		
	293	308	323	293	308	323
K_0	4.1953	4.9239	5.7432	3.7747	4.1822	4.586
ΔG^0 (KJ mol ⁻¹)	-3494.93	-4084.021	-4696.248	-3237.45	-3665.75	-4091.82
ΔH^0 (KJ mol ⁻¹)	8251.67			5110.43		
ΔS^0 (KJ mol ⁻¹ K ⁻¹)	40.0565			28.4778		

The negative value of the standard Gibbs free energy change and the positive standard entropy change suggest that the adsorption reaction was a spontaneous one. Also the positive standard enthalpy change confirms the assertion made in the beginning of this section: that the adsorption process is an endothermic reaction.

Competing effects

The effect of ionic Strength

As shown in in figure 11a and 11b, the presence of other metal ions in the metal ion solution affect the adsorption efficiency negatively as its concentration increases. The negative effect is also more pronounced depending on the metal ion in competition as it is observed that the adsorption efficiency of Ni^{2+} decreased, reaching 85%, 83%, 49% and 15% when in competition with 0.1M of Na^+ , K^+ , Ca^{2+} and Mg^{2+} respectively. For Co^{2+} the adsorption efficiency decreased to 83%, 84%, 10% and 1% when in competition with Na^+ , K^+ , Ca^{2+} and Mg^{2+} respectively.

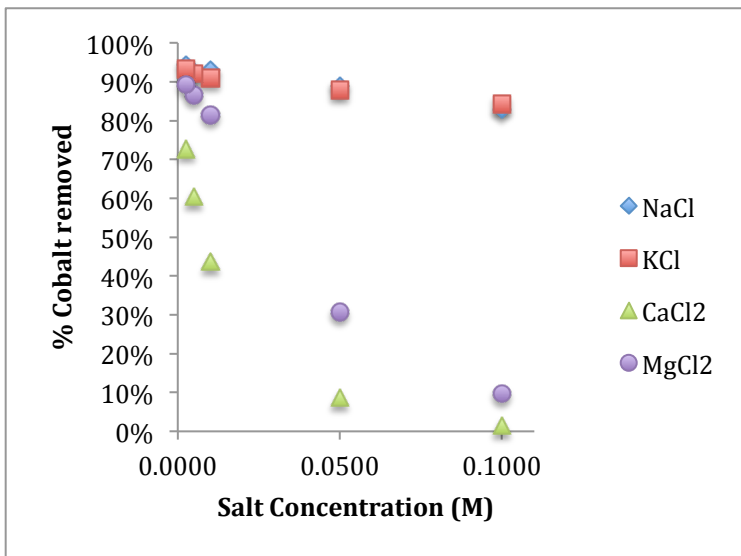


Figure 11A: Ionic Strength effect for cobalt adsorption.

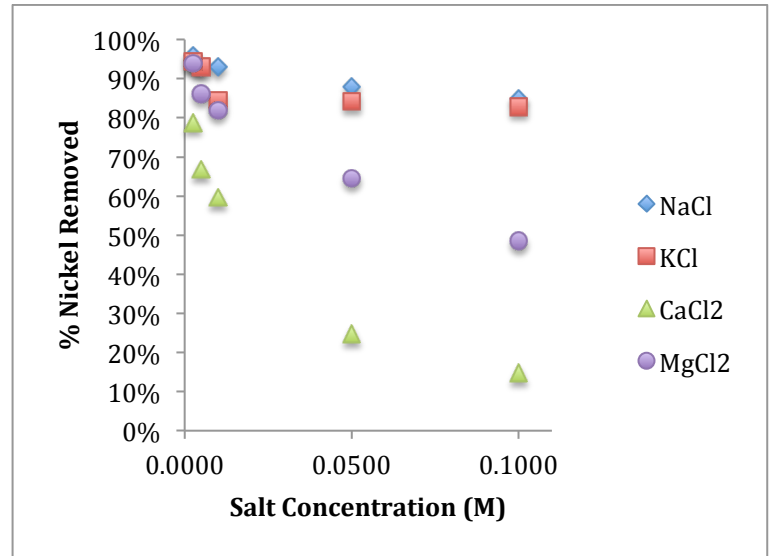


Figure 11B: Ionic strength effect for nickel adsorption.

The negative impact is mainly due to the metal ion competition for adsorption spaces (Hui et al, 2005). This effect can also be attributed to a number of factors mentioned below. First of all, the affinity between metal ions and Cl^- ions has an effect on adsorption efficiency of the adsorbent. The reduced adsorption efficiency could therefore be as a result of the formation of metal chloride (El-Bayaa et al, 2009), which reduces the amount of free metal ions available in solution for adsorption.

Secondly, the increase in salt concentration results in an increase in the ionic strength. This increase in ionic strength results in the increase in the ratio of chelation to ion exchange (El-Bayaa et al, 2009). Hence as the salt concentration increases there is a corresponding decrease in the ion exchange process, which results in a decrease in the adsorption efficiency. There is also decreasing activity of metal ions in solution due to increasing non-ideality of the solution with ionic strength (El-Bayaa et al, 2009).

Competition due to presence of both Nickel and Cobalt ions

Up to this point, the two metal ions of interest have been studied in isolation with the XG-CA-Na-A composite beads showing better adsorption results for the nickel ions than for the cobalt ions. Subsequently, it was important to know how the composite beads reacted when both metal ions were present in solution.

After running the experiments with both metal ions present in solution it was observed that the composite beads favored the cobalt ions slightly more than the nickel ions as shown in figure 12.

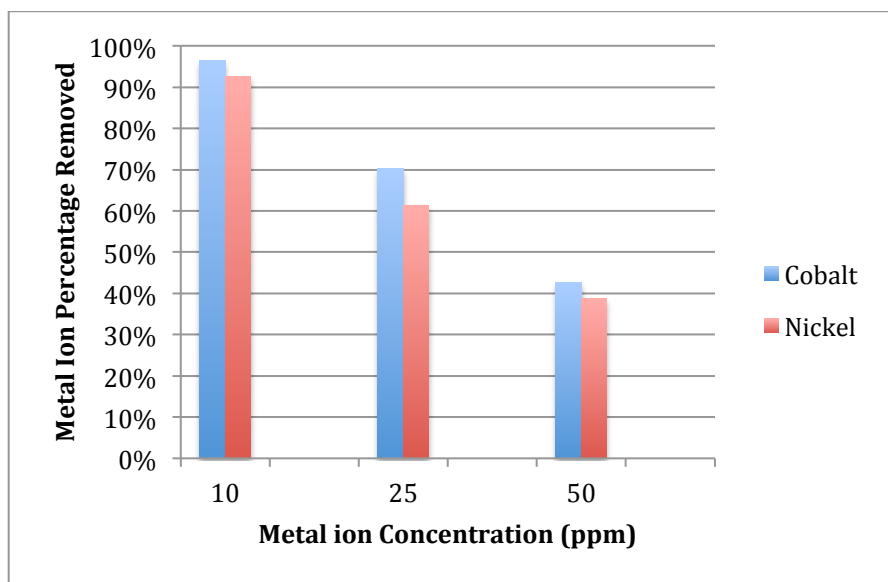


Figure 12: A comparison between the amount of nickel ions and cobalt ions removed from solution when both ions are present in solution.

This result is unexpected as the earlier results suggest that the XG-CA-Na-A composite beads are more efficient in adsorbing nickel atoms than they are in

adsorbing cobalt ions. The disparity can however be explained by looking closely at the free energy of hydration shown in table 7.

Table 7: The hydrated Ionic radii and Free energy of Hydration for the metal ions in solution.

Metal Ion	Ionic Radii (Hydrated) (nm)	Free Energy of Hydration (Kcal g ⁻¹ ion)
Co ²⁺	0.423	-479.5
Ni ²⁺	0.404	-494.2

(Volkov et. al, 1997) (Hui et. al, 2005)

Based on the free energy of hydration the metal with the highest free energy of hydration should prefer to remain in the solution phase (Hui et al, 2005). Hence even though the hydration ionic radii of the cobalt ion is greater than that of the nickel ion, there is still more cobalt available for adsorption than nickel and that therefore explains why more cobalt ions are adsorbed when both metal ions are present in solution.

XG-CA-Na-A beads performance in synthesized nuclear wastewater

As shown in figure 13, the XG-CA-Na-A composite beads removed 99.5% of the cobalt present and 98.3% of the Nickel present in the synthetic nuclear power wastewater solution.

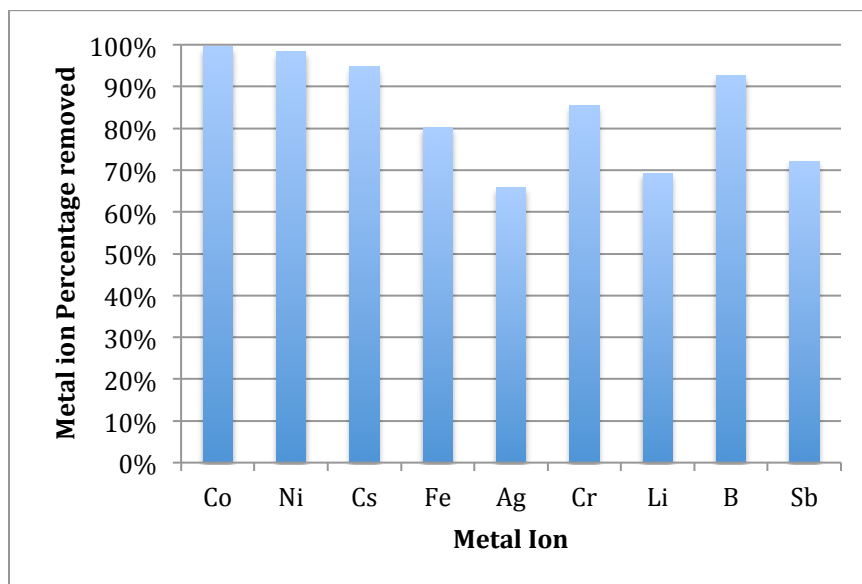


Figure 13: Plot showing the percentage removal of all metal ions present in the synthetic nuclear power plant wastewater solution

These results confirmed the XG-CA-Na-A composites' ability in treating real wastewater containing nickel and cobalt, as their removal percentages remain high even with the presence of other competing metal ions.

Comparisons between XG-CA-Na-A beads and other previously studied Adsorbents.

With the results obtained above the efficiency of the XG-CA-Na-A beads can only be qualified by comparing these results to results available for other potential adsorbents. As tables 7 and 8, the XG-CA-Na-A composites beads look promising with respect to Ni²⁺ and Co²⁺ adsorption since it had relatively high adsorption capacities in the treatment of wastewater containing low concentrations of Co²⁺ and Ni²⁺ ions.

Table 8: Comparison between XG-CA-Na-A composite beads and other adsorbents in removing nickel ions from solution

Nickel removal						
Material	C ₀ (mg L ⁻¹)	Dosage (g L ⁻¹)	Adsorption Capacity (mg g ⁻¹)	Condition	Reference	
XG-CA-Na-A	15	2.00	45.662	T=293K pH=5	This work	
GMZ Bentonite	2-24.03	0.50	14.396	T= 303K pH=5.4	(Yang et al, 2009)	
Oxidized Carbon Nanotubes	10-200	0.20	49.261	T= 293K pH=6	(Munther and Meunier, 2007)	
Modified Activated Carbon	25	5.00	37.175	T=293K pH=5	(Hasar, H, 2003)	
Seaweed	100	4.50	20.63	T=293K pH=4.5	(Vijayaraghavan et al, 2004)	
NFK-6 Zeolite	9.34	0.60	8.5202	T=293K pH=6.25	(Zhang et al, 2010)	
Bio-char	100	7.00	22.22	T=293K pH=7	(Murat et al, 2013)	

Table 9: Comparison between XG-CA-Na-A composite beads and other adsorbents in removing cobalt ions from solution

Cobalt removal					
Material	C_0 (mg L ⁻¹)	Dosage (g L ⁻¹)	Adsorption Capacity (mg g ⁻¹)	Condition	Reference
XG-CA-Na-A	15	2.00	25.575	T=293K pH=5.0	This work
Activated Carbon (Hazelnut shell)	45.55	5.00	13.879	T=298K pH=6.0	(Demirbas, 2003)
IRN77	100	2.00	86.17	T=298K pH=5.3	(S. Rengaraj and Seung-Hyeon, 2002)
SKN1	100	2.00	69.44	T=293K pH=5.3	(S. Rengaraj and Seung-Hyeon, 2002)
Seaweeds	100	4.50	18.58	T= 298K pH=4.0	(Yavuz et al, 2003)
Bio-char	100	4.00	28.09	T=293K pH=7	(Murat et al, 2013)

Also the wide range of pH values that the composites can operate effectively in and the ability to obtain relatively good results at room temperature makes the XG-CA-Na-A composites makes it a favourable adsorbent option as compared to the other options available.

CONCLUSION

The present study showed that the XG-CA-Na-A composite beads, which is easily available and can be easily prepared, were effective in removing both cobalt and nickel metal ions from aqueous solutions compared to many other adsorbents. It was discovered that the optimal condition for metal ion adsorption using these composite beads were at a pH of 5 and an adsorbent dosage of 2g L^{-1} . The study also revealed that the adsorptive capacity of the composite beads increased with increasing temperature. In terms of kinetics, the Pseudo-second-order model best described the adsorption kinetics and based on the Weber and Morris model the adsorption process is limited by both the film diffusion and particle diffusion step.

The Langmuir isotherm model best described the adsorption process and based on the thermodynamic study, the adsorption process is an endothermic reaction and a spontaneous one.

FUTURE PERSPECTIVES

Now that this project has verified that the XG-CA-Na-A composites can be effective adsorbents in the removal of heavy metals from nuclear power plant wastewater, it will be important to test the behavior of these beads in a column. The behavior and the effectiveness of the beads when they are in a pilot scale adsorption column will be necessary in order to effectively conclude on the viability of these composite beads as adsorbents in the industry.

REFERENCES

1. **Nuclear Power Plant Radioactive Water Remediation.** *New Logic Research, Inc. - Industries Water.* Web. 21 Sept. 2013.
<<http://www.vsep.com/industries/nuclear.html>>
2. S. Rengaraj, Seung-Hyeon Moon, **Kinetics of adsorption of Co (II) removal from water and wastewater by ion exchange resins,** *Water Research*, 2002, 36(7), pp. 1783-1793.
3. S. Babel, T.A. Kurniawan, **Cr(VI) removal from synthetic wastewater using coconut shell charcoal and commercial activated carbon modified with oxidizing agents and/or chitosan.** *Chemosphere*, 54 (7) (2004), pp. 951–967.
4. Fenglian Fu, Qi Wang, **Removal of heavy metal ions from wastewaters: A review,** *Journal of Environmental Management*, Volume 92, Issue 3, March 2011, pp 407-418.
5. Health and Ecological Criteria Division (HECD), Office of Science and Technology (OST), Office of Water (OW) for Office of Groundwater/Drinking Water (OGWDW), OW, United States Environmental Protection Agency (U.S. EPA). **Drinking Water Health Advisory for Boron and Compounds**, 2008.
6. United States Environmental Protection Agency (U.S. EPA). **Drinking Water Contaminants.** 3 June 2013. Web. 21 Sept. 2013.
<<http://water.epa.gov/drink/contaminants/index.cfm>>
7. United States Department of Natural Resources (US DNR). **Groundwater Quality Standards.** 2012. [Data file]. Retrieved from
http://docs.legis.wisconsin.gov/code/admin_code/nr/100/140.pdf
8. M.A. Barakat, **New trends in removing heavy metals from industrial wastewater,** *Arabian Journal of Chemistry*, Volume 4, Issue 4, October 2011, Pages 361-377 .
9. L.K. Wang, Y.T. Hung, N.K. Shamas (Eds.), **Chemical precipitation Physicochemical Treatment Processes**, vol. 3. Humana Press, New Jersey (2004), pp. 141–198.
10. Rahman et al, **Liquid Radioactive Wastes Treatment: A review,** *Water*, 12 May 2011, pp. 551-565.
11. Kurniawan, T.A., Chan, G.Y.S., Lo, W.H., Babel, S., **Physicochemical treatment techniques for wastewater laden with heavy metals.** *Chemical Engineering Journal* Vol. 118, May 2006., 83-98.
12. A.D. Dhale, V.V. Mahajani, **Studies in treatment of disperse dye waste: membrane–wet oxidation process.** *Waste Management*, Volume 20, Issue 1, February 2000, Pages 85-92.
13. Stephen R. Schulte, **A guide to lowering pollution and recovering valuable process constituents.** *Products Finishing*, September 2011. October 9th 2013. Retrieved from: <http://www.pfonline.com/articles/recoveryrecycling-methods-for-platers>

14. Sam Catalano, Jason Lawrence et al, **Adsorbers**, Encyclopedia of Chemical Engineering Equipment, 2005. October 9th 2013. Retrieved from: <http://encyclopedia.che.engin.umich.edu/Pages/SeparationsChemical/Adsorbers/Adsorbers.html>
15. Geoffrey L. Price, **What is a Zeolite?** Web. October 9th 2013. Retrieved from: http://www.personal.utulsa.edu/~geoffrey-price/zeolite/zeo_narr.htm
16. Zhang, S, Xu Fang, **Silica modified calcium alginate – xanthan gum hybrid bead composites for the removal and recovery of Pb(II) from aqueous solution**. Chemical Engineering Journal Vol. 234, September 2013, Pages 33-42.
17. K.S. Hui, C.Y.H. Chao, S.C. Kot, **Removal of mixed heavy metal ions in wastewater by zeolite 4A and residual products from recycled coal fly ash**, Journal of Hazardous Materials, Volume 127, Issues 1–3, 9 December 2005, Pages 89-101.
18. V.C. Srivastava, M.M. Swamy, I.D. Mall, B. Prasad, I.M. Mishra, **Adsorptive removal of phenol by bagasse fly ash and activated carbon: equilibrium, kinetics and thermodynamics**, Colloids Surf., A 272 (2006) 89–104.
19. K.Y. Foo, B.H. Hameed, **Insights into the modeling of adsorption isotherm systems**, Chemical Engineering Journal Vol. 156, January 2010, Pages 2-10.
20. C. Luo, R. Wei, D. Guo, S. Zhang, S. Yan, **Adsorption behavior of MnO₂ functionalized multi-walled carbon nanotubes for the removal of cadmium from aqueous solutions**, Chemical Engineering Journal Vol. 225, 1 June 2013, Pages 406–415.
21. D. Mohan, K.P. Singh, **Single-and multi-component adsorption of cadmium and zinc using activated carbon derived from bagasse-an agricultural waste**, Water Research Vol. 36, May 2002, Pages 2304–2318.
22. Halil Hasar, **Adsorption of nickel(II) from aqueous solution onto activated carbon prepared from almond husk**, Journal of Hazardous Materials, Volume 97, 28 February 2003, Pages 49-57.
23. Shitong Yang, Jiaying Li, Yi Lu, Yixue Chen, Xiangke Wang, **Sorption of Ni(II) on GMZ bentonite: Effects of pH, ionic strength, foreign ions, humic acid and temperature**, Applied Radiation and Isotopes, Volume 67, Issue 9, September 2009, Pages 1600-1608.
24. Zhang Hui, Xianjin Yu, Lei Chen, Yongjie Jing, Zhiwei Ge, **Study of Ni adsorption on NKF-6 zeolite**, Journal of Environmental Radioactivity, Vol 101, 24 September 2010, Pages 1061-1069
25. Munther Issa Kandah, Jean-Luc Meunier, **Removal of nickel ions from water by multi-walled carbon nanotubes**, Journal of Hazardous Materials, Volume 146, Issues 1–2, 19 July 2007, Pages 283-288.
26. Xue-Song Wang, Juan Huang, Huai-Qiong Hu, Jing Wang, Yong Qin, **Determination of kinetic and equilibrium parameters of the batch adsorption of Ni(II) from aqueous solutions by Na-mordenite**, Journal of Hazardous Materials, Volume 142, 2 April 2007, Pages 468-476.

27. Erhan Demirbas, **Adsorption of Cobalt (II) ions from Aqueous solution onto Activated Carbon Prepared from Hazelnut Shells**, Adsorption Science and Technology Vol. 21, 22 August 2003, Pages 951-963.
28. Ömer Yavuz, Yalçın Altunkaynak, Fuat Güzel, **Removal of copper, nickel, cobalt and manganese from aqueous solution by kaolinite**, Water Research, Volume 37, Issue 4, February 2003, Pages 948-952
29. M. Ruiz, C. Tobalina, H. Demey-Cedeño, J.A. Barron-Zambrano, A.M. Sastre, **Sorption of boron on calcium alginate gel beads**, Reactive and Functional Polymers, Volume 73, Issue 4, April 2013, Pages 653-657, ISSN 1381-5148,
30. **Solubility-Product Constants for compounds at 25°C**. Web. February 14th 2014. Retrieved from:
<https://www.chem21labs.com/reference/SolubilityProductConstant.pdf>
31. Murat Kılıç, Çisem Kırbiyık, Özge Çepelioğullar, Ayşe E. Pütün, **Adsorption of heavy metal ions from aqueous solutions by bio-char, a by-product of pyrolysis**, Applied Surface Science, Volume 283, 15 October 2013, Pages 856-862.
32. K. Vijayaraghavan, J. Jegan, K. Palanivelu, M. Velan, **Biosorption of cobalt (II) and nickel(II) by seaweeds: batch and column studies**, Separation and Purification Technology, 6 December 2004, Pages 53–59
33. A.A. El-Bayaa, N.A. Badawy, E. Abd AlKhalik, Effect of ionic strength on the adsorption of copper and chromium ions by vermiculite pure clay mineral, Journal of Hazardous Materials, Volume 170, Issues 2–3, 30 October 2009, Pages 1204-1209.
34. Cobalt – Co, Lenntech water treatment solutions. Web. March 6th 2014. Retrieved from: <http://www.lenntech.com/periodic/elements/co.htm>
35. Nickel – Ni, Lenntech water treatment solutions. Web. March 6th 2014. Retrieved from: <http://www.lenntech.com/periodic/elements/ni.htm>
36. Volkov, Adrian, Gourary, S. Paula, and D. W. Deamer, Two mechanisms of permeation of small neutral molecules and hydrated ions across phospholipid bilayers, Bioelectrochem. Bioenergetics 42:153-160, 1997. Retrieved from: http://www.electrobionics.org/ionic_radii.pdf

APPENDIX

Appendix A: pH of precipitation for 15 mg L⁻¹ cobalt and nickel aqueous solutions.

Cobalt solution

$$[\text{Co}^{2+}] = 15 \frac{\text{mg}}{\text{L}} * \frac{1\text{g}}{1000\text{mg}} * \frac{1\text{mol}}{58.933\text{g}} = 2.5453 * 10^{-4} \text{ mol L}^{-1}$$

$$K_{\text{sp}} = [\text{Co}^{2+}][\text{OH}^-]^2$$

Therefore:

$$1.3 * 10^{-15} = [2.5453 * 10^{-4}][\text{OH}^-]^2 \rightarrow [\text{OH}^-]^2 = \frac{1.3 * 10^{-15}}{2.5453 * 10^{-4}} = 5.1075 * 10^{-12}$$

$$\text{Hence } [\text{OH}^-] = \sqrt{5.1075 * 10^{-12}} = 2.25998 * 10^{-6}$$

$$\text{pOH} = -\log[\text{OH}^-] = -\log[2.25998 * 10^{-6}] = 5.64589$$

$$\text{Hence pH} = 14 - \text{pOH} = 8.35$$

Hence the pH of precipitation for the cobalt aqueous solution is **8.35**.

Nickel solution

$$[\text{Ni}^{2+}] = 15 \frac{\text{mg}}{\text{L}} * \frac{1\text{g}}{1000\text{mg}} * \frac{1\text{mol}}{58.6934\text{g}} = 2.5557 * 10^{-4} \text{ mol L}^{-1}$$

$$K_{\text{sp}} = [\text{Ni}^{2+}][\text{OH}^-]^2$$

Therefore:

$$6.0 * 10^{-16} = [2.5557 * 10^{-4}][\text{OH}^-]^2 \rightarrow [\text{OH}^-]^2 = \frac{6.0 * 10^{-16}}{2.5557 * 10^{-4}} = 2.3477 * 10^{-12}$$

$$\text{Hence } [\text{OH}^-] = \sqrt{2.3477 * 10^{-12}} = 1.5322 * 10^{-6}$$

$$\text{pOH} = -\log[\text{OH}^-] = -\log[1.5322 * 10^{-6}] = 5.81468$$

$$\text{Hence pH} = 14 - \text{pOH} = 8.19$$

Hence the pH of precipitation for the nickel aqueous solution is **8.19**.